

## Survey of the Quasielastic ( $p, n$ ) Reaction Induced by Polarized Protons

J. M. Moss,\* C. Brassard,† R. Vyse,‡ and J. Gosset

Département de Physique Nucléaire, Centre d'Études Nucléaires de Saclay, BP 2, 91190-Gif-sur-Yvette, France

(Received 19 May 1972)

The differential analyzing power,  $A(\theta)$ , was measured in the quasielastic ( $p, n$ ) reaction on  $^{11}\text{B}$ ,  $^{27}\text{Al}$ ,  $^{60}\text{Ni}$ ,  $^{116}\text{Sn}$ , and  $^{120}\text{Sn}$ . The energy of the incident polarized proton beam was 24.5 MeV except in the case of  $^{27}\text{Al}$  where it was 20.3 MeV. The  $A(\theta)$ 's were oscillatory with a large forward-angle maximum of  $\pm(0.25$  to  $0.35)$ . Distorted-wave Born-approximation calculations using a macroscopic model give reasonable agreement with the data for  $^{27}\text{Al}$  and  $^{60}\text{Ni}$ . For the Sn isotopes, good agreement is found when an isospin-dependent spin-orbit term is added to the form factor. The sign of this term agrees with that given by a simple model, but its magnitude is poorly determined due to optical-model ambiguities.

### I. INTRODUCTION

The excitation of isobaric analog states via the quasielastic (QE) ( $p, n$ ) reaction has been the subject of numerous experimental investigations since 1961 when analog states in heavy nuclei were first observed by Anderson and Wong.<sup>1</sup> Formally the existence of the QE ( $p, n$ ) reaction, which may be viewed as elastic scattering with isospin flip, can be traced to terms in the nucleon-nucleus optical potential multiplied by the operator  $\vec{\tau} \cdot \vec{T}$ , where  $\vec{\tau}$  and  $\vec{T}$  are, respectively, the isospin operators of the nucleon and the nucleus.<sup>2</sup> The isospin dependence of the optical potential has been a subject of considerable interest for many years. Although terms depending on  $\vec{\tau} \cdot \vec{T}$  have been sought in optical-model (OM) analyses of elastic proton and neutron scattering, it is now widely recognized that the QE ( $p, n$ ) reaction is a much more reliable means of investigating such terms.

When the real central part of the isospin-dependent optical potential,  $V_1(r)$ , is expressed according to the reformulated OM of Greenlees *et al.*<sup>3</sup> the interest in its nature becomes evident,

$$V_1(r) = 2(2T)^{-1/2} \int [\rho_n(r') - \rho_p(r')] V_\tau (\vec{T}' - \vec{T}) d^3r', \quad (1)$$

$\rho_n$  and  $\rho_p$  are the neutron and proton density distributions, respectively, and  $V_\tau$  is the isospin-dependent component of the nucleon-nucleon effective force. Thus the QE ( $p, n$ ) reaction should be sensitive to the relative distribution of neutrons and protons in nuclei. In addition to a real central potential, Satchler<sup>4</sup> has proposed that the isospin dependence of the OM may contain an imaginary term. We propose further, on the basis of quite general arguments (see Sec. V), that an isospin-dependent spin-orbit (SO) potential might be ex-

pected. In general then, we have

$$U_1(r)\vec{\tau} \cdot \vec{T}/A = [V_1(r, \alpha) + iW_1(r, \alpha) + V_{s1}(r, \alpha_s)\vec{L} \cdot \vec{S}] \vec{\tau} \cdot \vec{T}/A, \quad (2)$$

where the  $\alpha$ 's stand for all parameters required to specify the shapes of the various components of  $U_1$ .

To date for the QE ( $p, n$ ) reaction at the higher energies (20 MeV and above) only differential cross sections have been measured. Such data are quite useful in determining the shape and magnitude of  $V_1$ . Considerable ambiguity remains, however, with regard to  $W_1$ , and no information is available on  $V_{s1}$ . With the view that polarization data should provide significant new information about the isospin dependence of the optical potential, particularly about  $V_{s1}$ , we have made the first measurements of the differential analyzing power in the QE ( $p, n$ ) reaction induced by polarized protons. The targets chosen for this initial survey were  $^{11}\text{B}$ ,  $^{27}\text{Al}$ ,  $^{60}\text{Ni}$ ,  $^{116}\text{Sn}$ , and  $^{120}\text{Sn}$ .

### II. EXPERIMENTAL TECHNIQUES

To facilitate time-of-flight (TOF) measurements a new experimental area has been set up at the Saclay cyclotron. This is shown schematically in Fig. 1. After extraction from the cyclotron, the beam is brought to focus in the scattering chamber by two pairs of magnetic quadrupoles. Immediately preceding the chamber is a solenoid whose function is to rotate the axis of polarization through angles varying from 30 to 80°. The purpose of the rotation is to preserve the usual geometry where the spin is perpendicular to the reaction plane, while permitting the neutron detector to be moved freely above the level of the beam. This allows the detector to be placed above the shielding walls of the adjacent experimental areas. The detector

is supported and positioned by a movable crane. After the scattering chamber the beam passes through a polarimeter equipped with a thin polystyrene foil and two solid-state detectors placed at identical angles on opposite sides of the beam. The beam is then stopped by a thick graphite plate. The absolute beam polarization  $P$  was determined by degrading the beam energy to 15.7 MeV, where the analyzing power for  $^{12}\text{C}(p, p)^{12}\text{C}$  at  $45^\circ$  is known.<sup>5</sup>

Because available intensities of polarized beams are typically a factor of 100 smaller than for conventional beams, certain fundamental problems are encountered in using neutron TOF. First, since one usually measures TOF relative to a signal synchronized with the periodicity of the beam, there can be confusion of neutron groups whose TOF differ by the period  $\tau_c$ . To eliminate this problem the standard procedure has been to increase  $\tau_c$  to a convenient value, typically  $0.5 \mu\text{sec}$ . For cyclotrons this implies a 5–10-fold increase in  $\tau_c$  with a corresponding decrease in beam intensity. This is obviously undesirable when only 10–20 nA of beam is available initially. We choose to sidestep the problem of overlap by accepting limitations on both the dynamic range of neutron velocities and the TOF. This was accomplished, as is shown in Fig. 2, by choosing the flight path and detector threshold to avoid overlap only for neutrons from the QE ( $p, n$ ) reaction.

Additional problems arose due to the poor inherent time structure of the beam. As is the case for many cyclotrons not having single-turn extraction, the pulse width of the extracted beam was too large to be useful for TOF. The causes of the poor time structure and considerations involved in improv-

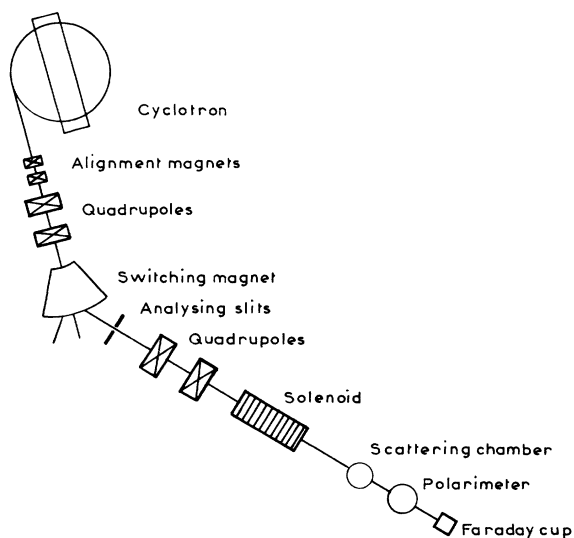


FIG. 1. Schematic layout of the experimental area.

ing it are complicated subjects and will not be discussed here. It is sufficient to say that, in agreement with similar findings in other laboratories, the pulse width could be improved by detuning the cyclotron slightly from the peak of the resonance. Considerable beam is sacrificed in this configuration. Reductions in intensity of 5 to 10 produced, on target, beams of 1 to 3 nA; the full width at half maximum of the beam was usually around 1.5 nsec. It was found that the off-resonance condition was quite stable over periods of 2 to 5 h.

It was necessary, because of the small beam intensity, to have a very large detector. Our detector consisted of three 5-cm-thick containers of NE213 liquid scintillator: The total volume was 1.8 liter. Light pulses from proton recoil events were detected by three 56 AVP photomultipliers, one on each container. The electronics required for recording TOF spectra is shown in Fig. 3. Because the cosmic-ray background was comparable to the counting rate of neutrons for the QE ( $p, n$ ) reaction some means of discrimination had to be devised. Fortunately NE213 liquid, common-

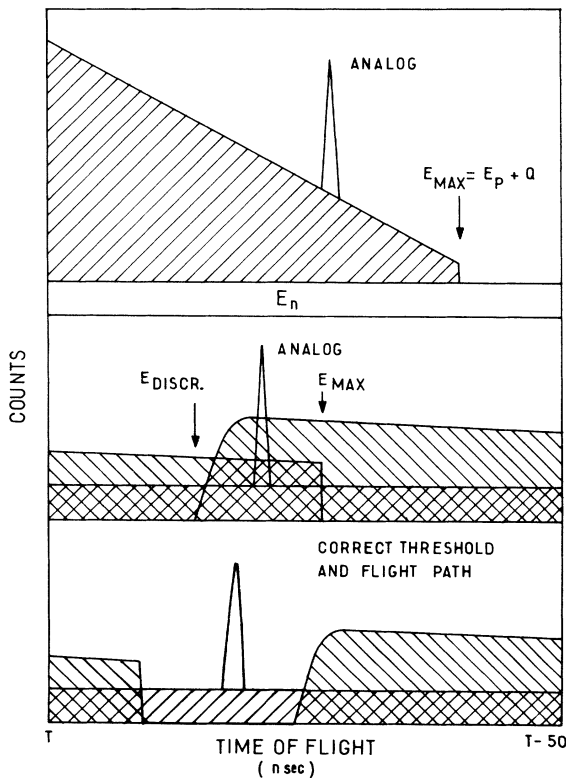


FIG. 2. Schematic energy spectrum of neutrons from the proton bombardment of a heavy nucleus. The center picture shows the problem of overlap in the TOF spectrum. The bottom picture shows the solution to this problem devised in the present experiment.

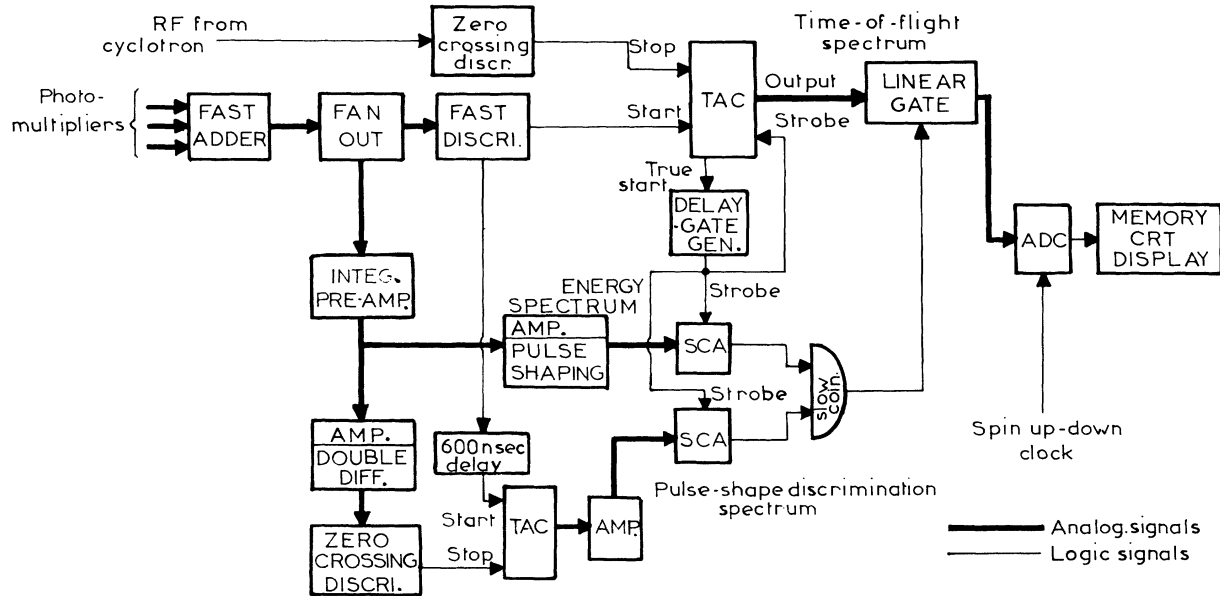


FIG. 3. The electronics setup used in the present experiment.

ly chosen for  $n$ - $\gamma$  discrimination, was also suitable for rejecting cosmic-ray muons on the basis of pulse-shape discrimination.

Counting times at each angle ranged from 1 to 10 h. The beam polarization was switched from up to down 5 times per second; the spectra were routed correspondingly in storage. The analyzing power derived from these experiments, defined in accordance with the Madison convention, is

$$A(\theta) = \frac{1}{P} \frac{N_+ - N_-}{N_+ + N_-},$$

where  $N_+$  is the number of counts recorded when the beam is polarized with spin up;  $N_-$  is defined analogously. Errors on the data points include only the statistical error in the data, neither the statistical (negligible) nor the systematic (5–10%) error in the determination of  $P$  were included.

### III. OPTICAL POTENTIALS

The nucleon-nucleus optical potential is commonly expressed as a sum of isospin-dependent and

TABLE I. Optical-model parameters used in the DWBA calculations. The  $(N-Z)/A$  dependence of the potentials is included in numbers given. For  $^{116}\text{Sn}$  parameter Sets 1 and 3 were taken from the global search of Becchetti and Greenlees (BG). Set 2 is an interpolation between Sets 1 and 3.

	$V_0$	$W_0$	$W_{D0}$	$V_{s0}$	$r$	$r_i$	$r_s$	$a$	$a_i$	$a_s$	Comment
$^{11}\text{B} + p$	56.6	0	9.2	5.5	1.15	1.15	1.15	0.57	0.5	0.57	
$^{11}\text{C} + n$	51.6	0	7.5	5.5	1.15	1.15	1.15	0.57	0.5	0.57	
$^{27}\text{Al} + p$	51.3	0	10.1	7.1	1.17	1.37	0.9	0.67	0.34	0.8	
$^{27}\text{Si} + n$	49.7	0	9.2	7.1	1.17	1.37	0.9	0.67	0.34	0.8	
$^{60}\text{Ni} + p$	50.6	2.7	6.5	6.2	1.17	1.32	1.01	0.75	0.56	0.75	
$^{60}\text{Cu} + n$	49.9	1.7	8.4	6.2	1.17	1.26	1.01	0.75	0.58	0.75	
$^{116}\text{Sn} + p$	53.6	2.7	7.3	6.2	1.17	1.32	1.01	0.75	0.61	0.75	Set 1; BG
$^{116}\text{Sb} + n$	49.5	0.8	8.63	6.2	1.17	1.26	1.01	0.75	0.58	0.75	Best fit
$^{116}\text{Sn} + p$	53.6	2.7	7.3	5.9	1.17	1.32	1.10	0.75	0.61	0.68	Set 2
$^{116}\text{Sb} + n$	49.5	0.8	8.63	6.4	1.17	1.26	1.10	0.75	0.58	0.68	
$^{116}\text{Sn} + p$	53.6	2.7	7.3	5.9	1.17	1.32	1.17	0.75	0.61	0.60	Set 3; BG
$^{116}\text{Sb} + n$	49.5	0.8	7.63	6.4	1.17	1.26	1.17	0.75	0.58	0.58	$r_s = r = 1.17$

-independent parts:

$$U(r) = U_0(r) + U_1(r)\vec{\tau} \cdot \vec{T}/A. \quad (3)$$

The operator  $\vec{\tau} \cdot \vec{T}$  has off-diagonal elements giving the QE ( $p, n$ ) reaction as well as diagonal elements affecting elastic scattering. Formally then, as pointed out by Lane,<sup>2</sup> one obtains coupled equations involving elastic scattering and the QE ( $p, n$ ) reaction. Fortunately, because the isospin-dependent term is a small part of the optical potential, the QE ( $p, n$ ) reaction can be approximately treated as being decoupled from elastic scattering and vice versa. The distorted-wave Born approximation (DWBA) can thus be used to describe this reaction. One does not, however, completely escape the effects of  $U_0$ , since optical potentials are needed in order to generate distorted waves for the incident proton and outgoing neutron. The optical parameters for  $^{60}\text{Ni}$  and  $^{116, 120}\text{Sn}$  are those obtained from the global analysis of Becchetti and Greenlees.<sup>6</sup> Unfortunately for light nuclei, where conventional OM analyses are beset by numerous problems, there is no global analysis available. We have chosen for  $^{27}\text{Al}$  the proton parameters found by Blair *et al.*<sup>7</sup> from an analysis of polarization and cross-section data at 20.3 MeV; the neutron parameters were derived from this set. For  $^{11}\text{B}$  the parameters are those given by Watson *et al.*<sup>8</sup> Table I lists all the parameter sets used in the present DWBA analysis. For  $^{116}\text{Sn}$ , additional sets

are given which will be discussed later.

There is, in principle, a question of consistency in a DWBA analysis of the QE ( $p, n$ ) reaction. For example, if one arbitrarily increases the strength of  $V_1$ , one should then change the proton and neutron distorting potentials, since the difference between these potentials is a reflection of the strength of the QE ( $p, n$ ) reaction. We have not taken the optical-model description of the  $(N-Z)/A$  dependence to be so exact as to demand complete consistency. Furthermore, arbitrary changes in the distorting potentials will change the predicted proton and neutron elastic scattering, and are therefore inconsistent with the DWBA. Thus, to avoid refitting the elastic scattering data for each DWBA calculation, we have used the best-fit proton and neutron potentials, discussed previously, irrespective of changes in either the strength or shape of  $U_1$ .

#### IV. MACROSCOPIC ANALYSIS

In the Lane model<sup>2</sup> the real and imaginary parts of  $U_1$  are usually assumed, without *a priori* justification, to have simple functional forms. We present first a series of calculations for all the targets in which  $U_1$  is assumed to be real or complex but without a spin-orbit term. The real part,  $V_1$ , is taken to have either a Woods-Saxon (WS) or WS derivative shape. The imaginary part,  $W_1$ , is assumed to have only a WS derivative shape. Geo-

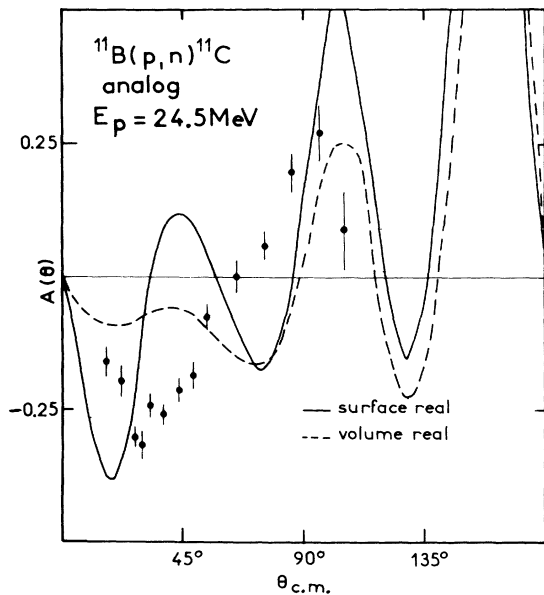


FIG. 4. Analyzing power in the QE  $^{11}\text{B}(p, n)^{11}\text{C}$  reaction. The curves are DWBA fits using macroscopic form factors.

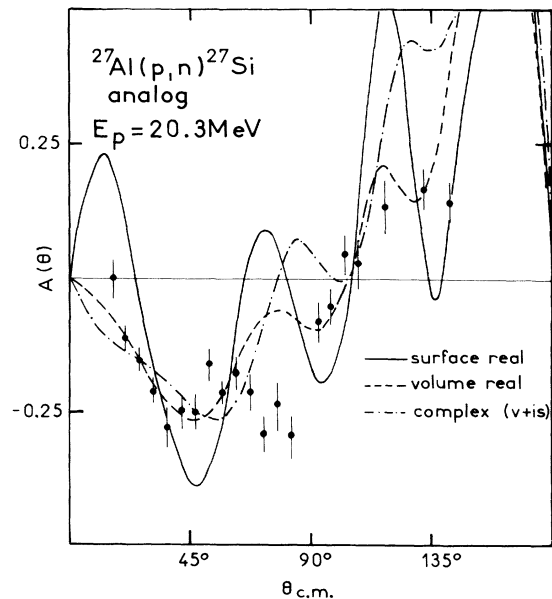


FIG. 5. Analyzing power in the QE  $^{27}\text{Al}(p, n)^{27}\text{Si}$  reaction. The curves are DWBA fits using macroscopic form factors. For the complex form factor  $V_1$  (volume) = 24 MeV;  $W_1$  (surface) = 12 MeV.

metrical parameters are the same as those given for the proton optical potentials in Table I.<sup>9</sup>

A.  $^{11}\text{B}(p, n)^{11}\text{C}$

In Fig. 4 it is seen that neither a volume nor a surface real form factor can account for the data. The addition of an imaginary component gives no improvement. There are a number of arbitrary adjustments of the parameters of both  $U_0$  and  $U_1$  which lead to better agreement with the data. However, in view of the usual shortcomings of the optical model for such light nuclei, no attempt was made to explore the parameter space systematically.

B.  $^{27}\text{Al}(p, n)^{27}\text{Si}$

From the curves in Fig. 5 it is clear that a volume real is favored over a surface real potential. The addition of an imaginary term to the volume real potential makes the fit slightly poorer. There is evidence for a second minimum around  $80^\circ$  which is not reproduced by the calculations.

C.  $^{60}\text{Ni}(p, n)^{60}\text{Cu}$

Due to a differential cross section which drops very steeply with increasing angle,  $A(\theta)$  could be obtained only for the most-forward angles. These angles suffice however to show that  $V_1$  must be of the surface form (see Fig. 6). The addition of an imaginary term does not improve the fit. Calculations were also made with a form factor composed of volume real and surface imaginary terms which was recently proposed by Carlson *et al.*<sup>10</sup> who ob-

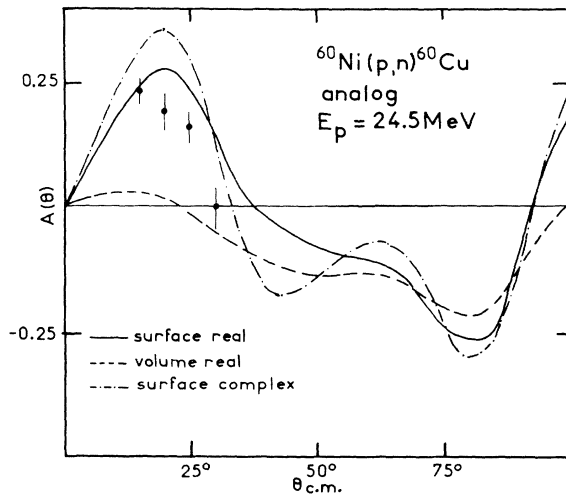


FIG. 6. Analyzing power in the QE  $^{60}\text{Ni}(p, n)^{60}\text{Cu}$  reaction. The curves are DWBA fits using macroscopic form factors. For the complex form factor  $V_1 = 9$  MeV;  $W_1 = 12$  MeV.

tain good fits to the  $^{58}\text{Ni}(p, n)^{58}\text{Cu}$  cross sections at  $E_p = 23$  MeV. This potential, being dominated by the real volume term, gives less than half the observed  $A(\theta)$  at forward angles.

D.  $^{116, 120}\text{Sn}(p, n)^{116, 120}\text{Sb}$

The analyzing powers of these reactions are identical within statistics. Figure 7 compares the  $^{116}\text{Sn}$  data with the prediction of the macroscopic model without a spin-orbit term in  $U_1$ . It is clear that none of the curves agrees with the data. Reasonable variations of the parameters  $U_1$  cannot reproduce the observed magnitude nor the phase of  $A(\theta)$ . At this point it is logical to consider the effect of a spin-orbit component in the isospin-dependent potential.

V. ISOSPIN-DEPENDENT SPIN-ORBIT POTENTIAL

There are simple reasons which would lead one to expect an isospin component in the nucleon-nucleus spin-orbit interaction. For example, as is shown by Satchler,<sup>4</sup> the real components of the optical potential may be schematically expressed as

$$\begin{aligned} V_0 &= \frac{1}{2}\rho(\bar{v}_{np} + \bar{v}_{pp}), \\ V_1 &= \frac{1}{2}\rho(\bar{v}_{np} - \bar{v}_{pp}). \end{aligned} \quad (4)$$

The quantities  $\bar{v}_{np}$  and  $\bar{v}_{pp}$  may be thought of as the

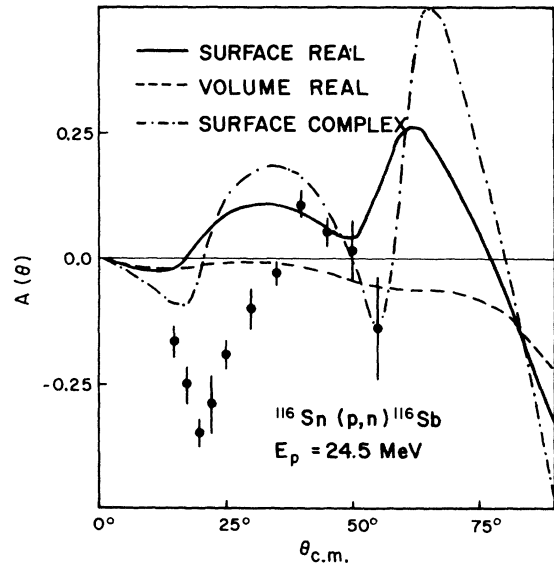


FIG. 7. Analyzing power in the QE  $^{116}\text{Sn}(p, n)^{116}\text{Sb}$  reaction. The curves are DWBA fits using macroscopic form factors. For the complex form factor  $V_1 = 9$  MeV;  $W_1 = 12$  MeV.

average contribution of the two-nucleon interaction in the  $p$ - $n$  and  $p$ - $p$  system, respectively, to the optical potential for protons. Since the central part of the two-body force is stronger in the  $n$ - $p$  system than it is in the  $p$ - $p$  or  $n$ - $n$  systems, one would expect  $V_1$  to be positive for protons and negative for neutrons. For the spin-orbit component,  $V_{s1}$ , we propose an analogous argument. It is well known, in the case of free nucleon scattering, that there is a strong spin-orbit force in the triplet-odd state.<sup>11</sup> In the limit of a very short range, then, the only contribution of this force comes from the state with  $L=1$ ,  $S=1$ , and  $T=1$ . For odd-parity states the  $p$ - $p$  and  $n$ - $n$  systems can only have  $S=1$ ,  $T=1$ , while the  $n$ - $p$  system can have, in addition,  $S=0$ ,  $T=0$  where the  $\vec{L} \cdot \vec{S}$  force does not contribute. Thus the spin-orbit interaction is twice as effective in the  $p$ - $p$  and  $n$ - $n$  systems as it is in the  $n$ - $p$  system. Evidence of this difference has been seen in microscopic calculations of analyzing powers in ( $p, p'$ ). Raynal<sup>12</sup> was able to explain differences between the  $2^+$  states of  $^{54}\text{Fe}$  and  $^{56}\text{Fe}$  using a two-body  $\vec{L} \cdot \vec{S}$  force.

Applying Eq. (4) to the spin-orbit interaction, if  $V_{s0}=6$  MeV then  $V_{s1}=-2$  MeV for protons on nuclei with  $N > Z$ . Arguments based on Eq. (4) are undoubtedly much too simple in the case of the spin-orbit force for any significance to be attached to the magnitude of  $V_{s1}$ . However, one should note that the sign of  $V_{s1}$  is opposite to that of  $V_1$ .

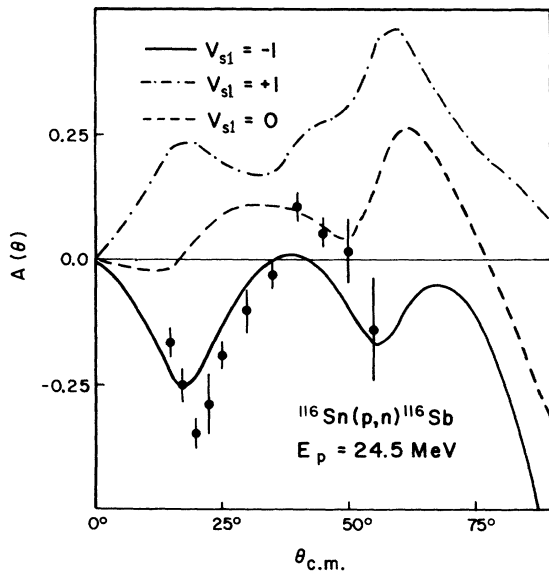


FIG. 8. DWBA fits using an isospin-dependent spin-orbit term in the form factor.  $V_{s1} = -1$  MeV means that the sign of this term is opposite to that of the real central term;  $V_1 = 9$  MeV.

For  $0^+$  to  $0^+$  QE transitions the inclusion of a one-body spin-orbit potential in the form factor is not difficult. The radial matrix element  $I_{J_a L_a J_b L_b}^{I s j}$  defined by Satchler<sup>13</sup> becomes

$$I_{J_a L_a J_b L_b}^{I s j} = (I_{J_a L_a J_b L_b}^{000} + \bar{L} K_{J_a L_a J_b L_b}^{000}) \delta_{J_a J_b} \delta_{L_a L_b} \quad (5)$$

with  $\bar{L} = \begin{matrix} L_a \\ -L_a + 1 \end{matrix}$  for  $J_a = L_a \pm \frac{1}{2}$ . The integral  $I$  includes the real and imaginary parts of  $U_1$ ; the integral  $K$  includes the radial form of  $V_{s1}$  which we take, for simplicity, to have a Thomas form,

$$V_{s1}(r) = \left( \frac{\hbar}{m \pi c} \right)^2 \frac{1}{r} V_{s1} \frac{df(r)}{dr} \vec{L} \cdot \vec{\sigma},$$

with

$$f(r) = (1 + e^x)^{-1}; \quad x = \frac{r - r_{s1} A^{1/3}}{a_{s1}}.$$

The geometrical parameters are taken to be the same as for  $V_1$ .

Figure 8 shows calculations with a real surface form factor to which has been added a term  $V_{s1}$  of two different signs; the curve with  $V_{s1}=0$  is reproduced from Fig. 7. It is clear that the only calculation which agrees with the data is that in which the components  $V_1$  and  $V_{s1}$  have opposite signs, in agreement with our simple model. It would be tempting at this point to conclude that  $V_{s1} \approx -1.5$  MeV. There are, unfortunately, ambiguities in

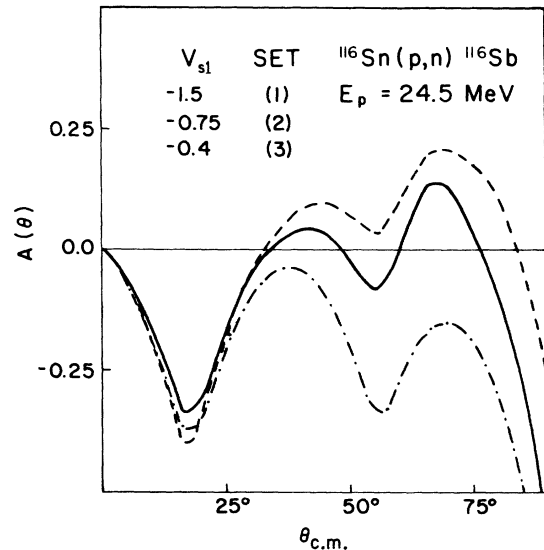


FIG. 9. Calculations using different strengths of  $V_{s1}$  in the form factor. The three curves illustrate the difficulty in determining the value of  $V_{s1}$  if  $V_{s0}$  is allowed to have large radii. Parameter Sets 1-3 are listed in Table I; the curves corresponding to Sets 1-3 are, respectively, dash-dot, solid and dash.

OM parameters which prevent one from drawing quantitative conclusions about  $V_{s1}$ . If one increases the radius of  $V_{s0}$  in the optical potentials for the distorted waves, the strength of  $V_{s1}$  can be diminished considerably while retaining the characteristic structure of the analyzing power. Figure 9 illustrates the problem. Parameter Set 3 in Table I was found by Becchetti and Greenlees<sup>6</sup> when the constraint  $r_s = r$  was imposed in their global search; Set 2 is an interpolation between Sets 1 and 3. The condition  $r_s < r$  has been found in numerous OM analyses. To the extent that this is believed one has some idea as to the magnitude of  $V_{s1}$ . If, on the other hand, one allows  $r_s \sim r$ , then it is possible to find a purely central surface-peaked form factor which approximately fits the data. At present we believe that parameter Set 2 with  $V_{s1} \sim -0.75$  MeV gives the best representation of the <sup>116</sup>Sn and <sup>120</sup>Sn data, however, it is obvious that more precise data over a wider angular range are necessary to specify quantitatively the isospin dependence of the spin-orbit potential.

It would be interesting to test the influence of the spin-orbit term in the case of <sup>60</sup>Ni, but our data are not sufficient to distinguish between calculations with or without this term. Moreover, the addition of a spin-orbit term has a very small effect on the predicted differential cross sections for <sup>60</sup>Ni and <sup>116</sup>Sn.

#### VI. SUMMARY

The first measurements of differential analyzing power have been reported for the QE ( $p, n$ ) reac-

tions on <sup>11</sup>B, <sup>27</sup>Al, <sup>60</sup>Ni, <sup>116</sup>Sn, and <sup>120</sup>Sn. At forward angles  $A(\theta)$  is negative for all targets except <sup>60</sup>Ni. The correct sign is reproduced by simple DWBA calculations. In terms of a macroscopic isospin-dependent optical potential the following conclusions can be drawn. For <sup>11</sup>B no satisfactory fit to  $A(\theta)$  was found. For <sup>27</sup>Al a volume real form factor gives a satisfactory fit to the data; for <sup>60</sup>Ni one must use a surface-peaked form factor. In the latter cases the imaginary component consistent with the data was less than a quarter of the real form factor. For the Sn isotopes a spin-orbit component of about  $\frac{1}{10}V_1$  is indicated in our calculations. The sign of  $V_{s1}$ , which is opposite to that of  $V_1$ , is consistent with a simple model of the origin of  $V_{s1}$ . However, owing to ambiguities in the optical model, quantitative conclusions about the magnitude of  $V_{s1}$  will require more precise data.

#### ACKNOWLEDGMENTS

The authors would like to express their appreciation to the technical staff of the Saclay cyclotron for designing and creating many of the components of the experimental system. In particular we want to thank C. Ré, R. Chaminade, J. Vergnaud, and C. Duriez. Thanks go also to J. Thirion for his support of the project and for numerous helpful suggestions, and finally to G. Greenlees for many discussions about the theoretical analysis.

Two of us (C.B. and R.V.) would like to thank the National Research Council of Canada for financial support during the course of this work.

\*Present address: School of Physics, University of Minnesota, Minneapolis, Minnesota 55414.

†Present address: Département de Médecine Nucléaire et de Radiobiologie, Centre Hospitalier Universitaire, Sherbrooke, Province de Québec, Canada.

‡Present address: Central Technical Division, MacMillan Broedel Ltd. P. O. Box 487, New Westminster, B.C., Canada.

<sup>1</sup>J. D. Anderson and C. Wong, Phys. Rev. Letters **7**, 250 (1961).

<sup>2</sup>A. M. Lane, Phys. Rev. Letters **8**, 171 (1962).

<sup>3</sup>G. W. Greenlees, G. J. Pyle, and Y. C. Tang, Phys. Rev. **171**, 1115 (1968); C. J. Batty, E. Friedman, and G. W. Greenlees, Nucl. Phys. **A127**, 368 (1969).

<sup>4</sup>G. R. Satchler, in *Isospin in Nuclear Physics*, edited by D. H. Wilkinson (North-Holland, Amsterdam, 1969).

<sup>5</sup>R. M. Craig *et al.*, Nucl. Instr. Methods **30**, 268 (1964).

<sup>6</sup>F. D. Becchetti and G. W. Greenlees, Phys. Rev. **182**, 1190 (1969).

<sup>7</sup>A. G. Blair *et al.*, Phys. Rev. C **1**, 444 (1970).

<sup>8</sup>B. A. Watson *et al.*, Phys. Rev. **182**, 977 (1969).

<sup>9</sup>C. Wong *et al.*, Phys. Rev. C **5**, 158 (1972). These authors propose using for  $U_1$  an average of the radius and diffuseness parameters of the proton and neutron optical potentials. In the present analysis the major change would be a reduction of the imaginary radius from 1.32 to 1.29. This produces a very small change in the predicted analyzing power.

<sup>10</sup>J. D. Carlson *et al.*, to be published.

<sup>11</sup>T. Hamada and I. D. Johnston, Nucl. Phys. **34**, 382 (1962).

<sup>12</sup>J. Raynal, in *Proceedings of the Third International Symposium on Polarization Phenomena in Nuclear Reactions, Madison, 1970*, edited by H. H. Barschall and W. Haerberli (The Univ. of Wisconsin Press, Madison, 1970).

<sup>13</sup>G. R. Satchler, Nucl. Phys. **55**, 1 (1964).